

Wave breaking velocity effects in depth-integrated models

Patrick J. Lynett

Department of Civil Engineering, Texas A&M University, College Station, TX 77843-3136, United States

Received 11 May 2005; received in revised form 25 August 2005; accepted 12 October 2005
Available online 21 November 2005

Abstract

A simple model for predicting the velocities under breaking waves in depth-integrated models is developed. A velocity modification due to wave breaking is formulated based on a specific exponential profile, which is then added to the numerically predicted, depth-integrated velocity profile. This modification is superficial in that it does not directly change the hydrodynamic calculations inside the depth-integrated model. The modifications can be employed in any of the numerous Boussinesq-type models, and is not dependant on the use of a particular breaking dissipation scheme. Horizontal velocity profiles, both mean and instantaneous, are compared with experimental data in the surf zone. The comparisons show good agreement, markedly better than the un-modified results, and on par with published numerical results from sophisticated models.

© 2005 Elsevier B.V. All rights reserved.

Keywords: Boussinesq; Undertow; Currents; Wave breaking

1. Introduction

For the near future, depth-integrated models will likely dominate nearshore, wave-resolving simulation, in particular when large spatial domains are considered. These models, primarily the shallow water and Boussinesq-type variety, predict the 3D wave field with 2D equations and so can simulate large basins in a practical length of computational time. While these properties seem to lead to great opportunities for nearshore hydrodynamic predictions, the depth-integrated derivation creates a set of equations for which some of the most important nearshore physics are approximated, or left out entirely.

Shallow-water-based depth-integrated models typically assume that the vertical profile of velocity can be represented by a polynomial, wherein the order of the polynomial is proportional to the accuracy of the resulting model. For non-breaking waves, this polynomial predicts the vertical profile of velocity very well, even for strongly nonlinear waves (e.g., Wei et al., 1995; Ryu et al., 2003), provided the wave is not in deep water. Implicit with this velocity profile, and often a direct inviscid assumption, is a lack of ability to simulate turbulence.

To simulate nearshore hydrodynamics, some method must be employed to approximate breaking, bottom friction, etc.

The depth-integrated model, in general, consists of one continuity equation, solved for the free surface elevation, and one vector momentum equation, solved for some characteristic velocity. To simulate the effects of breaking, the most common approach is to add a dissipation submodel to the momentum equation. This is an ad hoc addition, as common depth-integrated derivations start with an inviscid assumption, either implicitly or explicitly. There are two primary classes of breaking models: the roller model (e.g., Madsen et al., 1997) and the eddy viscosity model (e.g., Kennedy et al., 2000). The two models can be roughly equated, although the parameters controlling the dissipations are based on different physical thresholds.

Through a calibration of the parameters inherent in these models, very good agreement in wave height and mean water level can be achieved for wave transformation through the surf zone. Due to the success in applying the Boussinesq-type model through the surf, the natural progression is to employ these models for transport calculations. Transport calculations become very sensitive to accurate representation of the mean horizontal velocity, or undertow if below the mean trough level. It was immediately recognized that the raw Boussinesq model yielded very poor predictions of this undertow. For

E-mail address: plynett@tamu.edu.

example, when using a Boussinesq-type model, here the two-layer model of Lynett (*in press*), to predict the undertow of the Cox et al. (1995) experiment, the results prove poor. Shown in Fig. 1 are the numerical-experimental predictions. The numerical profiles are the wave-averaged horizontal velocities. As the numerical profiles are taken throughout the water column, the undertow (below the trough) must be balanced by the crest flux (above the trough). This should be the case with any finite amplitude wave theory — some undertow must be predicted.

Shown in the subplots at $x=3.5$ m and $x=5.8$ m, the numerical undertow agrees very well with the experimental. The reason for this is that at these locations, breaking has not yet initiated or has just barely initiated, and thus the impact on the profile due to breaking is minimal. These two plots are another demonstration of the ability of the Boussinesq model to simulate nearshore hydrodynamics accurately. Looking to the other four profiles shown, located throughout the surf zone, it is clear that the undertow is not predicted correctly in either magnitude or vertical variation. The Boussinesq profiles are always uniform below the trough, due to the Boussinesq-interpreted long wave, inviscid nature of the breaking wave.

Using the "raw" Boussinesq velocity profiles to predict the undertow leads to significant errors.

To work around this obstacle within the Boussinesq framework, researchers have developed solutions across a range of physical complexity. On the sophisticated end are the approaches similar to Veeramony and Svendsen (2000), who solved a coupled set of Boussinesq and vorticity models. This approach does involve the inevitable vorticity generation calibration, as well as a relatively complex equation model (compared to the standard Boussinesq), but yields very good agreement when compared to the undertow data of Cox et al. (1995).

Much of the work in examining Boussinesq velocity profiles in the surf zone employs the surface roller breaking model, used with the improved Boussinesq equations of Madsen et al. (1997). This particular model is somewhat limited in its ability to predict the vertical profile of velocity due to the manipulations of the model equations, rather than the velocity profile used to derive said equations (e.g., Nwogu, 1993). Due to these manipulations, a velocity profile consistent with the solved equations does not exist. However, in the surf zone, where Boussinesq predicted velocities are close to uniform in the

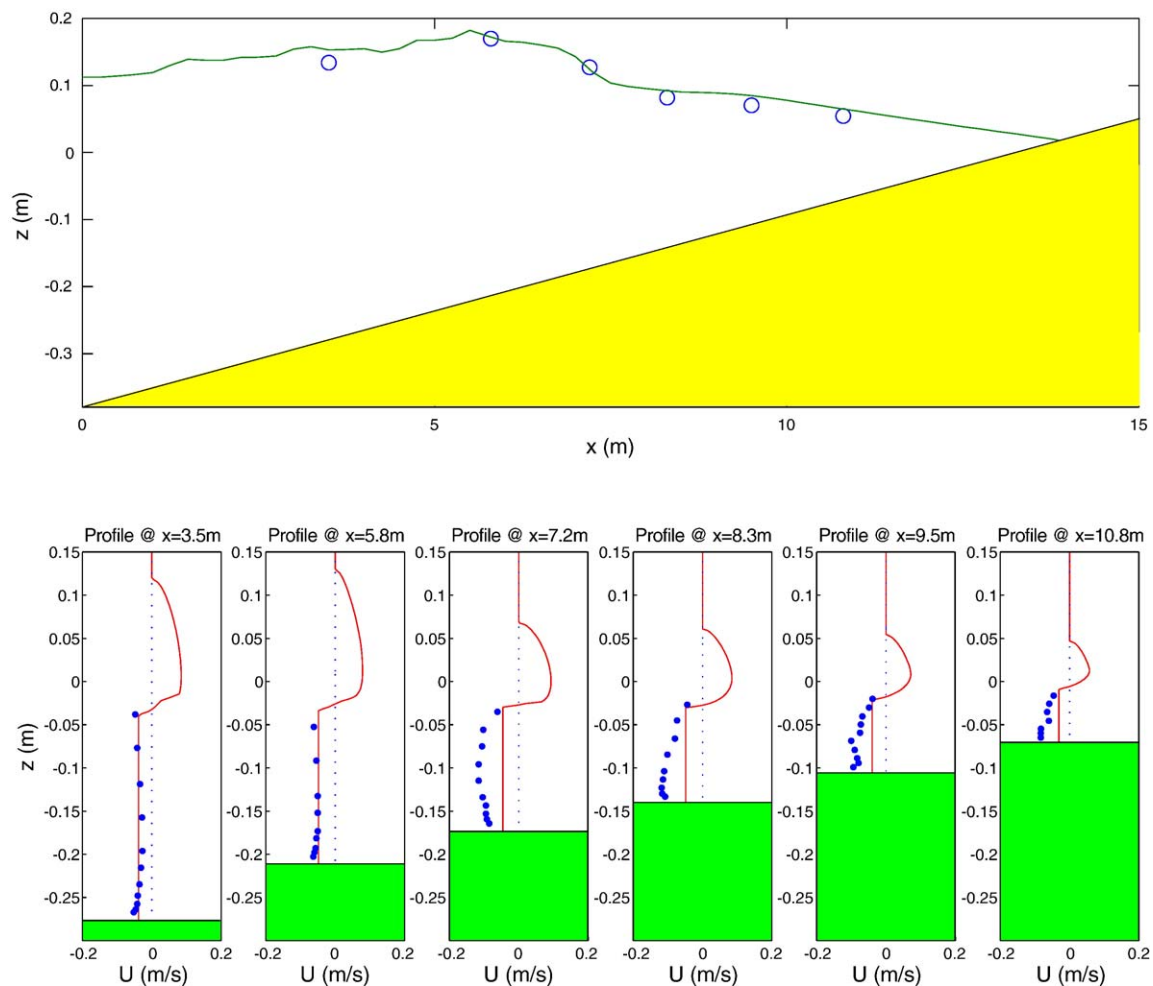


Fig. 1. Comparison with the data of Cox et al. (1995). Top plot is the numerical wave height profile (line) and the experimental (circles). The bottom row of plots are the time-averaged horizontal velocities at various locations, given in the subplot titles. The experimental values are shown with the dots, and the "unmodified" Boussinesq results by the solid line.

vertical, this limitation will not impact the results greatly. When using the roller breaking model, the horizontal velocity profile under a breaking wave is modified such that in the roller region, the velocity is assumed to be a large value related to the local long wave speed, while the velocity under the roller is set to a uniform value. This uniform value is determined such that the modified flux is equal to the Boussinesq-predicted flux. While this approach has been shown to yield reasonable results, it is not possible for this concept to predict a vertically varying undertow, as is measured in many experiments, without additional hydrodynamic submodels.

2. Breaker effect on depth-integrated velocity profile

A consistent modification to the velocity profile due to breaking is sought. In its foundation, the procedure given in this section is similar to the roller approach used to modify the vertical velocity profile, discussed above. Here, however, properties of the velocity modifications will be taken from the extended-Boussinesq theory.

Following the conventional perturbation derivation for Boussinesq equations, the vertical profile of the vertical velocity, W , is given in dimensionless form as:

$$W = -zS - T + O(\mu^2) \quad (1)$$

where

$$S = \nabla \cdot \mathbf{U}, \quad T = \nabla \cdot (h\mathbf{U}), \quad (2)$$

z is the vertical coordinate, \mathbf{U} is the vertically-varying horizontal velocity vector, and h is the local water depth. To include the impact of breaking induced velocity profile changes, a fundamental modification is made to the above velocity profile:

$$W = -zS - T + A(x, y, t)f(x, y, z, t) + O(\mu^2) \quad (3)$$

where A and f comprise some arbitrary function which is meant to approximately account for breaking effects. Using this modified vertical velocity, the horizontal velocity vector, as referenced to a velocity at an arbitrary elevation, is given by:

$$\begin{aligned} \mathbf{U} = \mathbf{u} - \mu^2 \left\{ \frac{z^2 - z_\alpha^2}{2} \nabla S + (z - z_\alpha) \nabla T \right\} \\ + \mu^2 \left\{ \nabla A \left[\int f(z) dz - \int f(z_\alpha) dz \right] \right. \\ \left. + A \left[\int \nabla f(z) dz - \int \nabla f(z_\alpha) dz \right] \right\} + O(\mu^4) \quad (4) \end{aligned}$$

where \mathbf{u} is the horizontal velocity evaluated at some arbitrary elevation z_α . The purpose of the additional terms in the horizontal velocity profile will be to allow velocities near the free surface to be larger when breaking is occurring, to better represent the fast moving breaking region. It is desired that

$\mathbf{U}(x, y, \zeta, t) = \mathbf{C}(x, y, t)$ where \mathbf{C} is some prescribed free surface breaking velocity and ζ is the free surface elevation. Further, let us define the Boussinesq predicted free surface velocity

$$\mathbf{u}_s = \mathbf{u} - \mu^2 \left\{ \frac{\zeta^2 - z_\alpha^2}{2} \nabla S + (\zeta - z_\alpha) \nabla T \right\} + O(\mu^4). \quad (5)$$

Therefore, a solution to the following expression is desired:

$$\begin{aligned} \mu^2 \nabla A \left[\int f(\zeta) dz - \int f(z_\alpha) dz \right] \\ + \mu^2 A \left[\int \nabla f(\zeta) dz - \int \nabla f(z_\alpha) dz \right] = \mathbf{C} - \mathbf{u}_s \quad (6) \end{aligned}$$

Using the assumption that $\nabla f(z) = O(\mu^2)$, employing $f(z_\alpha) = f(z_B) + O(\mu^2)$ where z_B is some elevation in the water column, and the substitution $g = \int f dz$, a relatively simple equations results

$$g(\zeta) - g(z_B) = 1 \quad (7)$$

where ∇A has been set equal to $\frac{\delta}{\mu^2} (\mathbf{C} - \mathbf{u}_s)$, and $\delta = 1$ when breaking is occurring and is 0 otherwise. As the initial modifications to the vertical velocity profile are ad hoc in nature, there is no guidance contained directly in the depth-integrated derivation as to what form $g(z)$ should take. Since the Boussinesq-model should capture the velocities correctly if the phenomenon is of the shallow- or intermediate-water type, we chose here to give g a deep-water based form, an exponential:

$$g = B e^{k(z-\zeta)} \quad (8)$$

where B is a coefficient and k is some vertical wave number. Substituting this form into (7) gives the solution for B :

$$B = \frac{1}{1 - e^{k(z_B - \zeta)}} \quad (9)$$

and we are left with the wave number, k , and the elevation, z_B , as unknowns. From this point on, all terms will be discussed in their dimensional form. To summarize, the modified horizontal velocity profile is given as:

$$\mathbf{U} = \mathbf{U}_O + \mathbf{U}_B \quad (10)$$

where

$$\mathbf{U}_O = \mathbf{u} - \left\{ \frac{z^2 - z_\alpha^2}{2} \nabla S + (z - z_\alpha) \nabla T \right\} \quad (11)$$

$$\mathbf{U}_B = \nabla A [g(z) - g(z_B)] \quad (12)$$

$$\nabla A = \delta (\mathbf{C} - \mathbf{u}_s) \quad (13)$$

It is noted that (10) is written in a more generic form using \mathbf{U}_O . While the derivation up to this point has looked at the “extended” Boussinesq model, it is completely applicable to any Boussinesq-type of model, for example depth-averaged or multi-layer. In these cases, only the expression for \mathbf{U}_O in (11) would change.

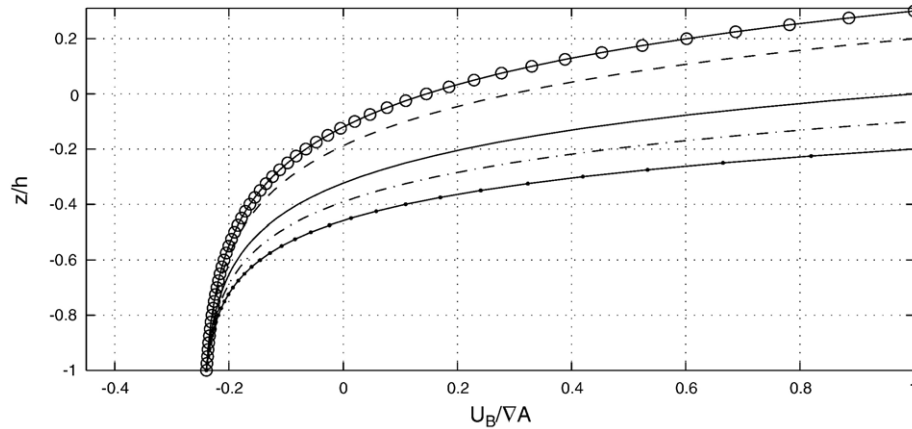


Fig. 2. Horizontal velocity modifications due to breaking, where the line with open circles is for $\zeta=0.3 h$, the dashed line for $\zeta=0.2 h$, the solid line for $\zeta=0$, the dashed–dotted line for $\zeta=-0.1 h$, and the solid dotted line for $\zeta=-0.2 h$.

With any modification of the velocity profiles comes a modification to the resulting depth-integrated continuity and momentum equations. The additional flux terms in the continuity equation are

$$\int_{-h}^{\zeta} \nabla A [g(z) - g(z_B)] dz = B \nabla A \left[\frac{1}{k} (1 - e^{-kH}) - H e^{k(z_B - \zeta)} \right] \quad (14)$$

where $H = \zeta + h$. Now, to solve the continuity equation, some value for k must be given. There are a few possibilities here, for

example, k can be related somehow to the total water depth, i.e., $k = 2\pi/H$, or based on some other instantaneous wave property, i.e., $k = \sqrt{|\zeta_{xx}/\zeta|}$ where x is the direction of propagation of the breaker. A value of k will be chosen that yields good agreement with experiment — it will be the empirical parameter of the breaking velocity modifications. With a given k , we are left with z_B as the remaining unspecified variable. Here, a choice is made for z_B based on experience when using the Boussinesq model for breaking wave studies. It is seen that the “unmodified” model, when using either a roller or eddy–viscosity breaker submodel in the momentum equation, reproduces mean quantities (wave height, mean free surface, etc.) in the surf

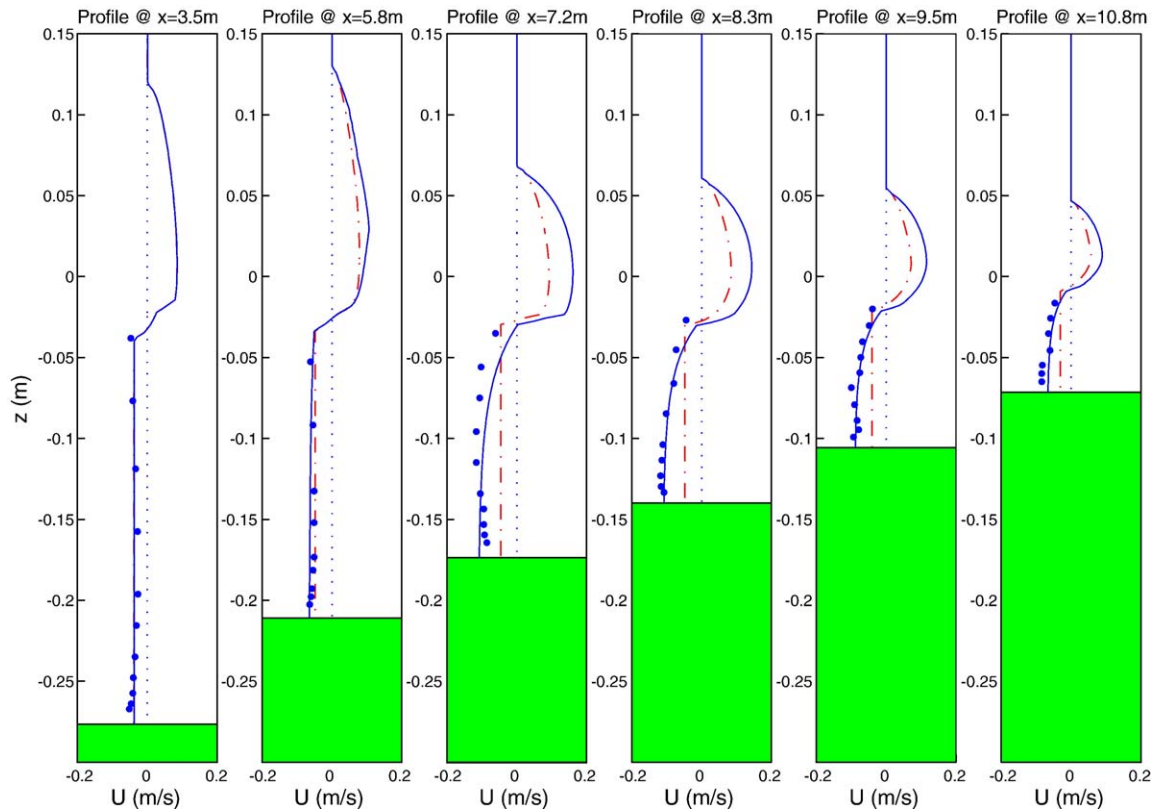


Fig. 3. Comparison with the data of Cox et al. (1995), using the same setup as in Fig. 1. The experimental values are shown with the dots, the breaking-enhanced Boussinesq by the solid line, and the unmodified Boussinesq results by the dashed–dotted line.

accurately. Thus the flux predicted by the “unmodified” model is already well predicted. We will chose z_B such that the new terms do not change the flux, i.e.,

$$\int_{-h}^{\zeta} \nabla A [g(z) - g(z_B)] dz = 0 \tag{15}$$

or

$$e^{-kH} + kHe^{k(z_B - \zeta)} = 1 \tag{16}$$

The above equation is readily solved for z_B :

$$z_B = -h + \frac{\ln[\frac{1}{kH}(e^{kH} - 1)]}{k} \tag{17}$$

Therefore, with a specified value of k , z_B is given and the breaking modifications to the velocity profile in (10) can be calculated. In the limit of very small k (long wave), the modifications resemble a linear trend going from a velocity addition at the free surface to a velocity subtraction near the bed, with z_B approaching $-h+H/2$, the midpoint of the instantaneous water column. For large k , the modification is a

velocity addition highly localized at the surface and a small velocity subtraction in the remaining water column, with z_B approaching ζ .

Looking to the momentum equation, additional terms will also be present when carrying through the modified velocity profiles. The assumption is made that the breaking submodels have already taken these terms in account in some approximate form. Thus, it can be concluded that the modifications given by (10) are in fact the implied velocity profile changes associated with the use of a breaking submodel, here the eddy viscosity model. In addition, since the changes presented here do not affect the governing equations, all previous free surface benchmarks and calibrations remain unchanged, and, in essence, the velocity profile changes in (10) are a post-processing modification.

3. Comparison with experimental data

The modified velocity profile under breaking waves will be compared with the available experimental data in this section. The data of Cox et al. (1995) and Ting and Kirby (1995, 1996), for both mean flows (undertoe) and phase-averaged velocities,

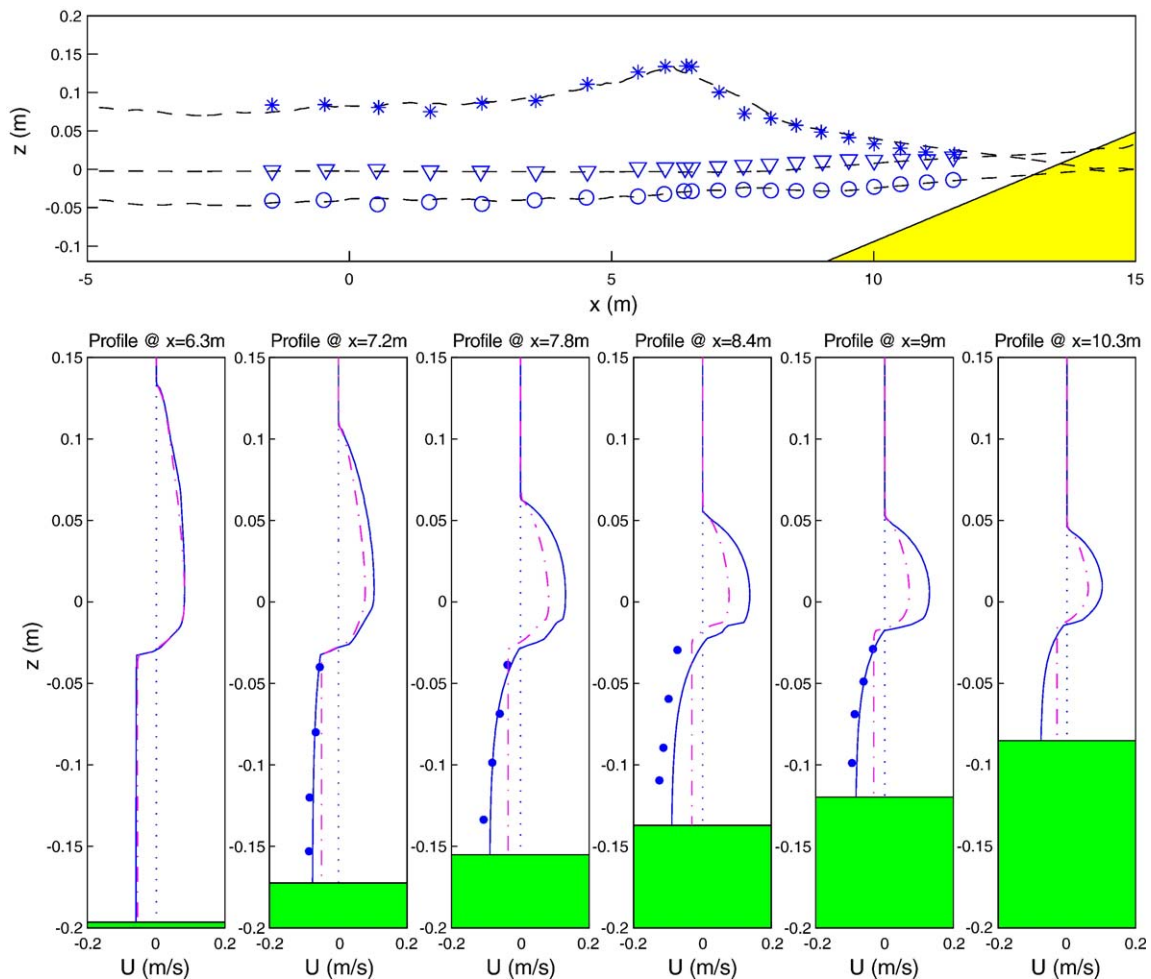


Fig. 4. Comparison with the data of Ting and Kirby spiller. The top plot shows the mean crest level (stars), mean water level (triangles), and mean trough level (circles) for the experiment as well as the numerical simulation. The lower subplots are the time-averaged horizontal velocities, where the experimental values are shown with the dots, the breaking-enhanced Boussinesq by the solid line, and the unmodified Boussinesq results by the dashed–dotted line.

is used. To achieve the best possible agreement with the data, the following value of k is specified:

$$k = \frac{5}{H} \tag{18}$$

The solutions are not strongly sensitive to this choice, with numerator values ranging from 4 to 6 yielding similar results. Note that the numerator value, as well as the chosen form of k , are chosen based on the model employed here, and may be different for other Boussinesq-type models. To elucidate how the added terms to (10) will modify the profile, Fig. 2 gives U_B for various free surface elevation values. At the free surface, an addition is made such that the velocity is equal to C , where

$$C = \frac{u_s}{|u_s|} \sqrt{\text{gravity} * H + \bar{U}}, \tag{19}$$

the nonlinear long wave speed corrected for the depth-averaged current, \bar{U} . Downward through the water column, the velocity addition decreases until the modifications act to reduce the velocity. Note that these curves will collapse if plotted against $(z - \zeta)/H$ instead of z/h , following the $\zeta = 0$ curve given in Fig. 2.

For the Boussinesq simulations, the highly-nonlinear, extended Boussinesq model is used for all simulations. A close variation of the eddy-viscosity model is employed to approximate wave breaking, as described in Lynett (in press). As a first experimental comparison, the data of Cox et al. (1995) is examined. Remember that this data has already been compared with the "unmodified" model, as shown in Fig. 1. The unmodified model, while capturing the mean velocity correctly near the trough level, shows significant errors below the trough. With the breaking velocity "enhancements", the mean velocities are predicted very well, as shown in Fig. 3. Both the magnitude and the vertical variation of undertow are captured throughout the surf zone. For this case, the breaking enhancements are large, leading to big differences in the two results, and indicating that for this wave, the Boussinesq predicted free surface velocity is much less than the nonlinear long wave speed. The agreement shown here is on par with published comparisons, based on more physically robust and computationally expensive formulations (e.g., Veeramony and Svendsen, 2000).

Next, the data of Ting and Kirby, for spilling (1995) and plunging (1996) breakers, is compared. These experiments

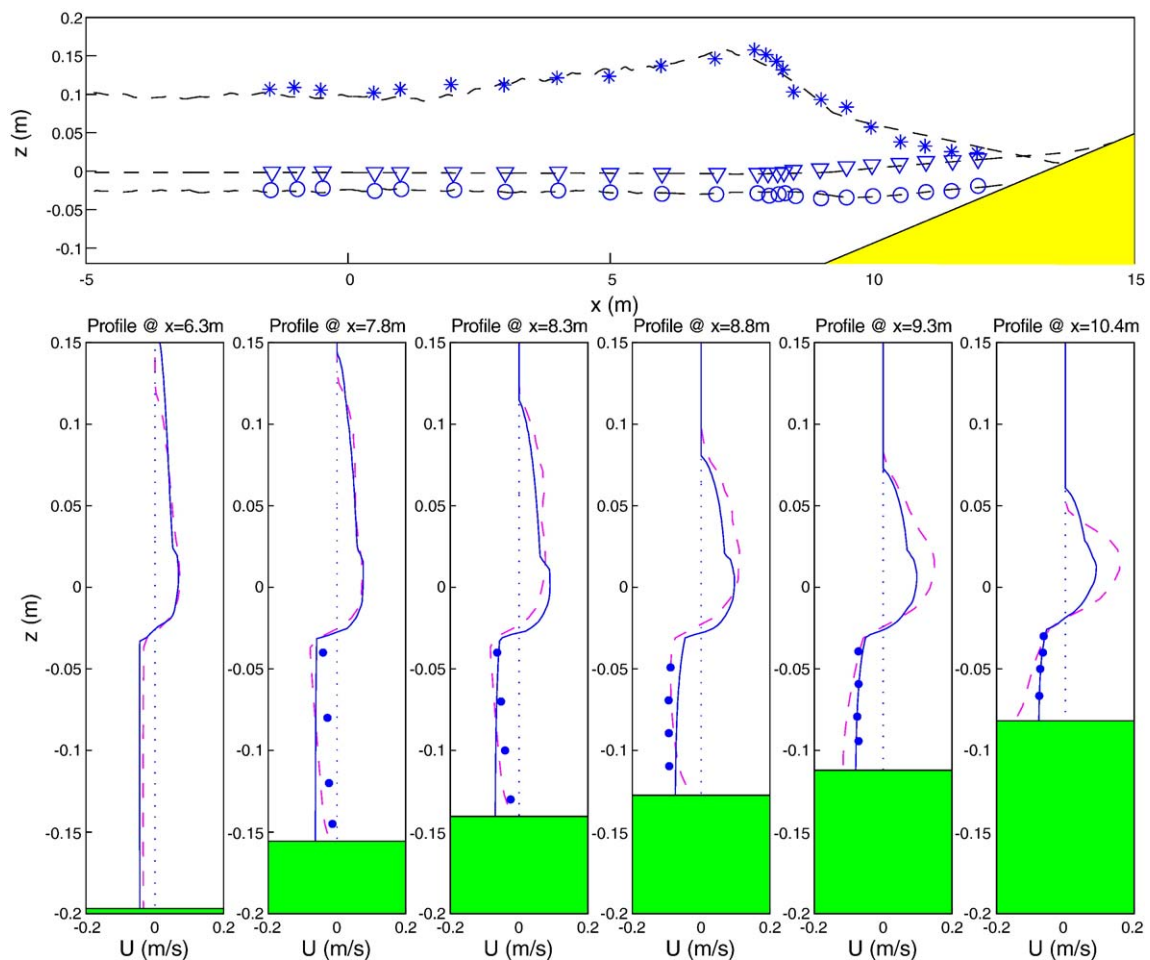


Fig. 5. Comparison with the data of Ting and Kirby plunger. The top plot shows the mean crest level (stars), mean water level (triangles), and mean trough level (circles) for the experiment as well as the numerical simulation. The lower subplots are the time-averaged horizontal velocities, where the experimental values are shown with the dots, the breaking-enhanced Boussinesq by the solid line, and the results of a VOF RANS model (COBRAS, provided by Dr. P. Lin) by the dashed line.

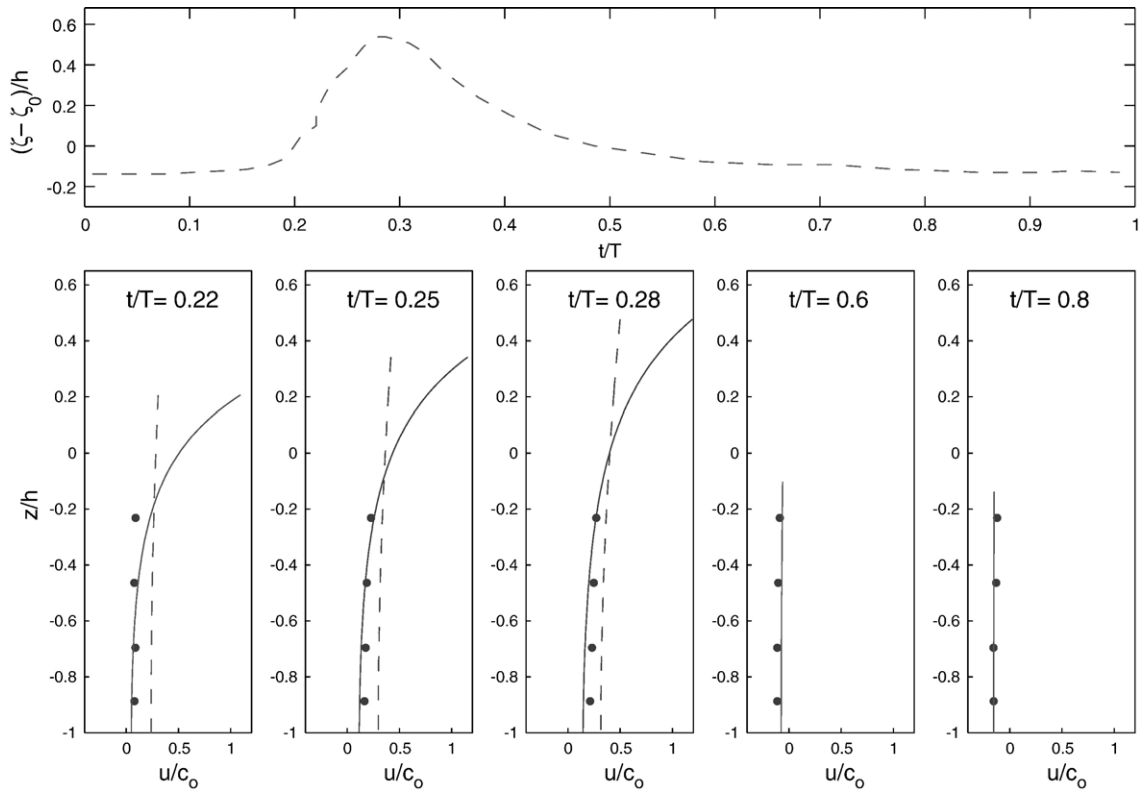


Fig. 6. Comparisons of the vertical profile of phase-averaged horizontal velocity at different wave phases for the Ting and Kirby spiller at $x=7.2$ m. The top plot shows the experimental phase-averaged free surface. In the lower subplots are the velocity profiles at different points under the wave, where the dots are the experiment, the breaking-enhanced Boussinesq by the solid line, and the unmodified Boussinesq results by the dashed line. Velocity in the lower plots is scaled by c_0 , the linear long wave speed.

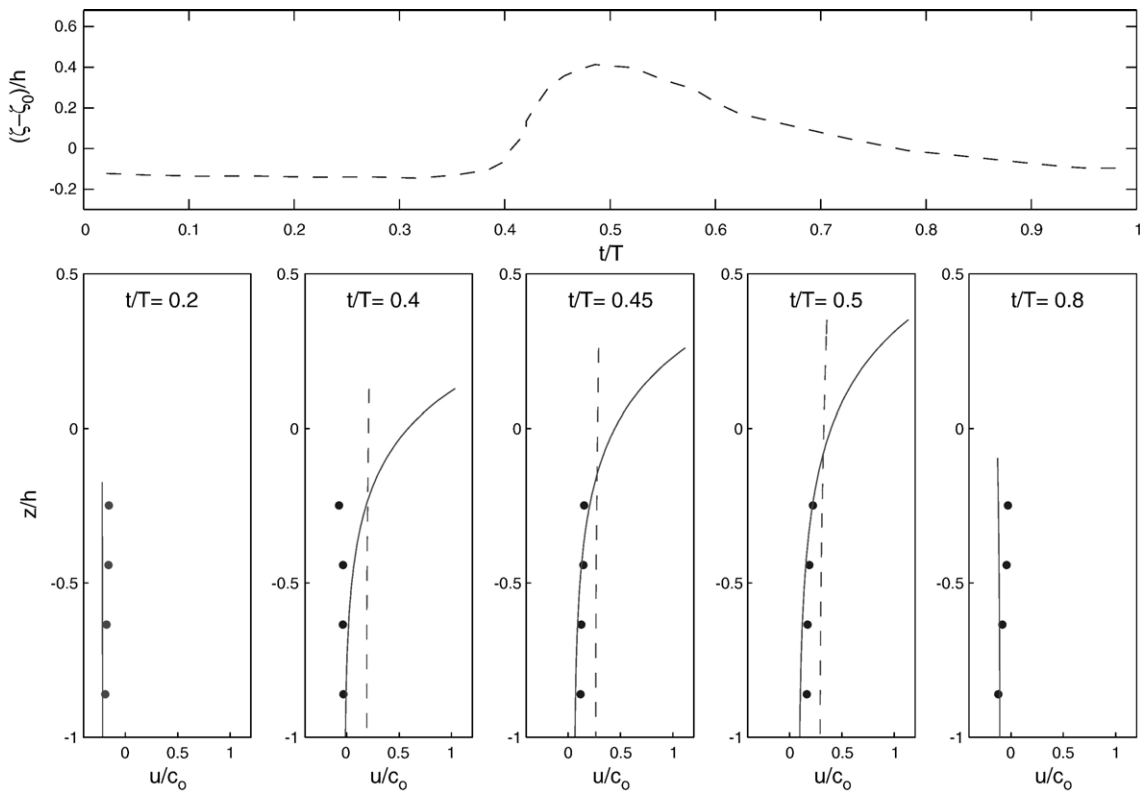


Fig. 7. Comparisons of the vertical profile of phase-averaged horizontal velocity at different wave phases for the Ting and Kirby spiller at $x=7.8$ m. Figure setup same as Fig. 6.

look at cnoidal wave breaking on a 1/35 slope. First, mean velocity profiles are discussed. In Fig. 4 are comparisons at four locations along the slope. As with the Cox et al. data, velocity measurements below the trough are available. The breaking enhanced model does a much better job at representing the undertow profile, including the vertical variation. The agreement at $x=8.4$ m is poor, although equal to the agreement achieved in other models (e.g., Lin and Liu, 2004). As with the data of Cox et al., the breaking enhanced model predicts a very different undertow profile as compared to the unmodified model.

A physical setup that does not show much difference between the breaking enhanced and unmodified models is that of Ting and Kirby (1996) for plunging cnoidal waves. For this comparison, shown in Fig. 5, the breaking enhanced model is compared with the experimental and the numerical results from a RANS VOF model, COBRAS (Lin and Liu, 1998). Before breaking, at $x=6.3$ m, the predictions of the two numerical models through the entire water column are in agreement. In the outer surf zone, the RANS model predicts the undertow better, capturing the vertical variation. Also note that at these locations, the positive mass flux, above the trough level, as predicted by the two models are in very close agreement. Moving towards the inner surf, the Boussinesq breaking enhanced model yields a much better prediction of the undertow, with excellent agreement at the two innermost measurement locations. The breaking enhanced impact for this case is in fact rather small, as can be inferred from the small vertical variation of the undertow predicted by this model. This

implies that the Boussinesq prediction of the free surface velocity of the breaker is near the nonlinear long wave speed.

While examination of the undertow profiles indicates that the breaking enhancements are correctly modifying the velocity profiles in the mean sense, it does not necessary require that the instantaneous profiles are being altered reasonably. To investigate this point, the data of Ting and Kirby (1995), for the spiller, is re-examined. The experimental velocity profiles are phase-averaged, which is the equivalent of the instantaneous Boussinesq velocity profile, where turbulent fluctuations are not modelled. Figs. 6–8 give comparisons at three locations, $x=7.2$, 7.8, and 9 m, respectively. In the top plot of each of these figures is the free surface elevation (waveform) for one wave period.

Looking to the vertical profiles of horizontal velocity, given in the lower subplots of the figures, it becomes clear that while the breaking enhancements have been shown to predict undertow well, they also capture the phase-averaged velocities below the mean trough level. Given in each figure are three profiles under the breaking part of the wave, and two elsewhere. Note that the unmodified profiles are close to vertically invariant at all locations under the wave. Only at the trough of the wave, however, is this a good approximation. The breaking enhancements show a large improvement over the unmodified predictions, with the vertical variation and the velocity magnitude very well modelled. It is also evident that below the trough level, the proposed modification will act to reduce the horizontal velocity under the breaker, thereby generally decreasing the skewness (and asymmetry) of the

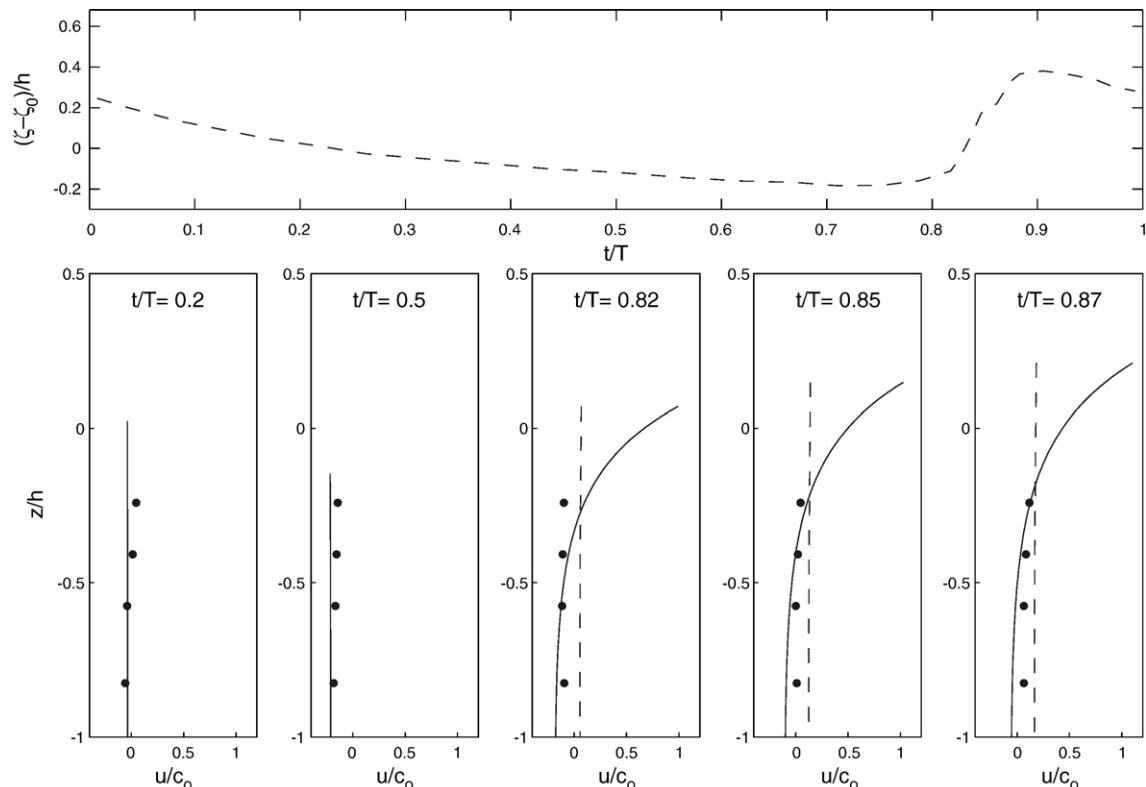


Fig. 8. Comparisons of the vertical profile of phase-averaged horizontal velocity at different wave phases for the Ting and Kirby spiller at $x=9.0$ m. Figure setup same as Fig. 6.

under-trough velocity. The effect is opposite above the trough. This incorrect under-trough prediction in the unmodified Boussinesq model has been recognized previously; for example see the “roller” velocity modification in some Boussinesq models (commonly in the Madsen et al. (1997) type Boussinesq models, see developments by Rakha (1998)). To reiterate, the unmodified Boussinesq model is capturing the depth-averaged velocity well at all locations — but the vertical variation is missing under the breaking portion. This observation served as the spark for the research presented here.

4. Conclusions

A simple model for predicting the velocities under breaking waves in depth-integrated models is developed. Under the non-breaking portions of the wave, no modification is made to the Boussinesq vertical profiles of velocity. The velocity modification is formulated based on a specific exponential profile, which is then added to the numerically predicted velocity profile under a breaking wave. This modification is superficial in that it does not directly change any of the hydrodynamic calculations inside the depth-integrated model. However, if one were to employ these modifications in a model that used the velocity for transport predictions through the surf and swash, the predictions would be different. The modifications can be employed in any of the numerous Boussinesq-type models, and is not dependant on the use of any of the existing breaking dissipation schemes. It is reiterated here that much of the benefit of this “breaking enhancement” comes from its simplicity and ability to be seamlessly integrated into existing models.

While the established experimental data with which to compare these modifications is limited, the results are promising in both the average and instantaneous sense. The approach presented here could be extended to the boundary layer as well, or, alternatively, one could use a more physically detailed approach (e.g., Liu and Orfila, 2004). Extension of this approach to 2HD is also straightforward, although additional and ongoing research into the inclusion of vertical vorticity evolution is equally important for velocity profile modeling. With accurate velocity profiles both in magnitude and vertical

variation, such as those given here, using established Boussinesq-type models, without additional viscous sub-models, to simulate transport in the surf zone becomes a more promising endeavor.

Acknowledgement

The research presented here was partially supported by a grant from the National Science Foundation (CTS-0427115).

References

- Cox, D.T., Kobayashi, N., Okayasu, A., 1995. Experimental and numerical modeling of surf zone hydrodynamics. Technical Report CACR-95-07. Center for Applied Coastal Research, University of Delaware.
- Kennedy, A.B., Chen, Q., Kirby, J.T., Dalrymple, R.A., 2000. Boussinesq modeling of wave transformation, breaking and runup: I. One dimension. *Journal of Waterway, Port, Coastal, and Ocean Engineering* 126, 39–47.
- Lin, P., Liu, P.L.-F., 1998. A numerical study of breaking waves in the surf zone. *Journal of Fluid Mechanics* 359, 239–264.
- Lin, P., Liu, P.L.-F., 2004. Discussion of vertical variation of the flow across the surf zone. *Coastal Engineering* 50, 161–164.
- Liu, P.L.-F., Orfila, 2004. Viscous effects on transient long wave propagation. *Journal of Fluid Mechanics* 520, 83–92.
- Lynett, P., in press. Nearshore wave modeling with high-order Boussinesq-type equations. *Journal of Waterway, Port, Coastal and Ocean Engng.*
- Madsen, P.A., Sorensen, O.R., Schaffer, H.A., 1997. Surf zone dynamics simulated by a Boussinesq-type model. Part I. Model description and cross-shore motion of regular waves. *Coastal Engineering* 32, 255–287.
- Nwogu, O., 1993. Alternative form of Boussinesq equations for nearshore wave propagation. *Journal of Waterway, Port, Coastal, and Ocean Engineering* 119 (6), 618–638.
- Rakha, K.A., 1998. A quasi-3D phase-resolving hydrodynamic and sediment transport model. *Coastal Engineering* 34, 277–311.
- Ryu, S., Kim, M.H., Lynett, P., 2003. Fully nonlinear wave–current interactions and kinematics by a BEM-based numerical wave tank. *Computational Mechanics* 32, 336–346.
- Ting, F.C.-K., Kirby, J.T., 1995. Dynamics of surf-zone turbulence in a strong plunging breaker. *Coastal Engineering* 24, 177–204.
- Ting, F.C.K., Kirby, J.T., 1996. Dynamics of surf-zone turbulence in a spilling breaker. *Coastal Engineering* 27, 131–160.
- Veeramony, J., Svendsen, I., 2000. The flow in surf zone waves. *Coastal Engineering* 39, 93–122.
- Wei, G., Kirby, J.T., Grilli, S.T., Subramanya, R., 1995. A fully nonlinear Boussinesq model for surface waves: Part 1. Highly nonlinear unsteady waves. *Journal of Fluid Mechanics* 294, 71–92.